STUDY OF SPECTRAL, OPTICAL, THEORETICAL, DIELECTRIC AND MECHANICAL PROPERTIES OF NEWLY SYNTHESISED OPTICALLY ACTIVE SEMIORGANIC SINGLE CRYSTAL-BISGLYCINE STRONTIUM CHLORIDE

[1]K. Amudha, [2]R. Mohan Kumar, [3]P. R. Umarani
[1]Associate Professor, [2]Assistant Professor, [3]Joint Director (Retd)
[1]Department of Physics,
[1]R.M.D Engineering College, Kavaraipettai-601 206, India,

Abstract: Bisglycine Strontium Chloride (BGSC), a semi-organic newly synthesised crystal obtained by slow evaporation solution growth technique (SEST) using aqueous solution at ambient temperature. The unit-cell parameters of the grown crystal were confirmed by single crystal XRD. FTIR studies have been carried out for analysing the presence of functional groups. The transparency of the grown crystal was identified by the UV-Vis spectrum. The dielectric constant (ε_r) and dielectric loss ($\tan\delta$) as a function of frequency were measured for the grown crystal. The solid state parameters such as valence electron energy, plasma energy, Penn gap and Fermi energy were evaluated theoretically by using the empirical relation. The mechanical stability of the grown crystals was studied using Vickers micro hardness tester. The estimated values were used to calculate the electronic polarizability.

Index Terms- Slow evaporation, linear optical, Tauc's plot, Mechanical, Dielectric, Penn analysis.

I.INTRODUCTION

Due to rapid advancement in science and technology, application of single crystal plays a prominent role and has unbounded limits. In these single crystals, there exists an ordered array of atoms which shows characteristic symmetry. Hence many Scientist groups, all around the world focuses on production of high quality NLO single crystals with reasonable size. Like semiconductors operating on electrons these materials operates on light. In recent past, second and higher harmonic generating semi organic materials have fascinated much interest due to their ubiquitous applications such as frequency conversion, high-speed information processing, optical communications, optical data storage, optical disc data storage, medical imaging, spectroscopic image processing, colour display and optical communication [1,2]. Compared with organic NLO materials, the semi-organic materials has extended transparency region-down to UV, chemical inertness, large non-linearity, high resistance to laser induced damage, low angular sensitivity, and good mechanical hardness [3]. Amino acids and their complexes belong to a family of organic and semi-organic materials that have been considered for photonic applications [4]. Glycine (NH_2CH_2COOH) is one such amino acid that crystallizes in six different forms: α, β, γ, β, ε and β.. α-glycine has no asymmetric carbon atom and is optically inactive. It has been reported that α-glycine combines with H_2SO_4 , $CaCl_2$, $CaNO_3$, $BaCl_2$, and $AgNO_3$ [5-11] to form useful single crystals. The aim of this paper is to report the growth of BGSC crystals by the slow evaporation method and to present the results of different studies such as single-crystal x-ray diffraction (SCXRD) studies, UV–visible NIR transmittance studies, Fourier transform infrared (FTIR) spectral studies, theoretical studies, dielectric studies, and Vickers microhardness studies.

II. EXPERIMENTAL PROCEDURE

2.1. Crystallization

Commercially available analar grade glycine, (CH_2NH_2COOH) strontium chloride ($SrCl_2 \cdot 6H_2O$) were used in this crystallization process using double distilled water as solvent.. In the first stage of slow evaporation solution growth technique the glycine and strontium chloride were taken in 2:1 stoichiometric ratio and mixed using double distilled. The resultant solution was stirred well for more than 5 hrs continuously using a magnetic stirrer to attain saturation. The solubility of compounds was found to increase with increase of temperature. The prepared solution was filtered carefully using Whatman filter paper, transferred to clean crystallizers and allowed to evaporate at room temperature. During this process, the crystallizers were covered with perforated polyethylene sheet and kept in a dust free chamber and closely monitored. The crystallization took place in this natural isothermal evaporation method within 20-30 days. Colourless and the transparent, good quality crystals of size 0.8x0.5x0.2cm^3were harvested. Photograph of as grown crystal were shown in Fig.1.

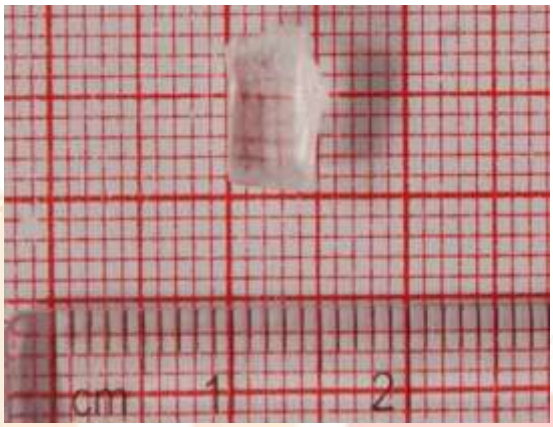

Figure.1 Photograph of as grown crystal

2.2 Characterization studies

The single crystal X-ray diffraction (XRD) analysis was carried out using Bruker X8 Kappa APEXII spectrometer (USA) to study its unit cell dimensions. CHN analysis was studied using Elementer Vario EL III with detection ranges 0.004-30 mg abs (or 100%).The UV-VIS-NIR transmittance spectrum was assessed using Varian, Cary 5000 with the wavelength range of 175-2300 nm to determine its optical transmittance and band gap by means of Tauc's plot. Transparent and good quality crstals were selected for dielectric studies in the frequency range 50 Hz- 5 MHz using HIOKI 352-50 LCR HITESTER at different temperatures. The Vicker hardness,fracture toughness, brittleness index and elastic stiffness constant were calculated using MATSUZAWA MMTZ-7 (Singapore) series.

III. RESULTS AND DISCUSSION

3.1. Single crystal X-ray diffraction

Single crystal x-ray diffraction studies reveals the crystalline nature of the title compound and the lattice parameters obtained were tabulated in Table 1, indicates that the grown crystal belongs to orthorhombic crystal system with non-centrosymmetic space group Pbcm, which consent with previous report [12] displaying SHG activity.

The expected chemical reaction is as shown in Eq. (1)

$$SrCl_2 + 2\ CS(NH_2) \rightarrow Sr[CS(NH_2)_2]2Cl_2 \quad (1)$$

The synthesized salt was purified by several re-crystallizations.

Table 1

Crystallography data of BGSC crystal

Parameters	Reported data[12]	Grown crystal data
a	16.2206 Å	16.24 Å
b	9.3116 Å	9.34 Å
c	8.2478 Å	8.25 Å
α	90°	90°
β	90°	90°
γ	90°	90°
Cell Volume	1245.75 $Å^3$	1252 $Å^3$
Crystal system	Orthorhombic	Orthorhombic
Space group	Pbcm	Pbcm
Colour	Colourless	Colourless

3.2 CHN analysis

To substantiate the presence of thiourea in the title semiorganic material, CHN analysis was carried out and the acquired result shows that the formed compound contains the following percentage N=7.64%, C=12.73%, S=ND and H=4.63%.

3.3 EDAX analysis

EDAX analysis conducted on the grown crystal confirms the presence of elements in Strontium, Chlorine, oxygen, Nitrogen and carbon as shown in Table 2 and Fig.2.

Table 2

List of elements present in the grown crystal

Element	Line Type	Wt%	Atomic %
C	K series	27.5	35.28
N	K series	14.71	16.19
O	K series	47.61	45.86
Al	K series	0.29	0.16
Cl	K series	2.94	1.28
Sr	L series	6.94	1.22
	Total:	100	100

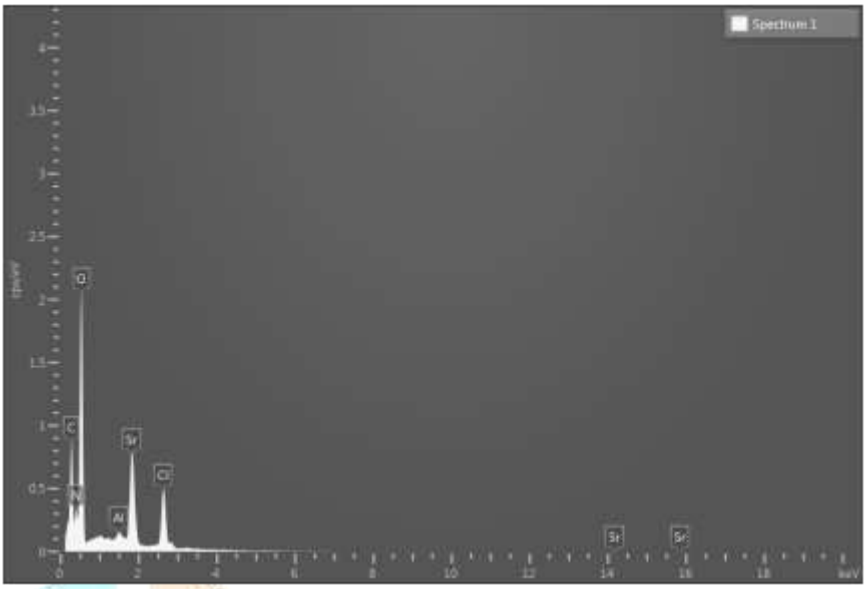

Fig. 2 EDAX spectrum

3.3 UV-VIS NIR spectral analysis

The optical transmission and absorption spectrum of BGSC single crystal of 3mm thick in the spectral range of 200-2500 nm is depicted in Fig 3. The exceeding high transparency is the vital parameter for materials to show signs of NLO properties. The lower cut-off wavelength is originated to be 213 nm, the sample possesses good transmission and lesser absorption in the entire visible region believed to be most appropriate for SHG [13-14] and also for optical device fabrications [15-16].

The optical absorption coefficient (α) was deliberated from transmittance using the following relation [17],

$$\alpha = \frac{2.303}{d}\log\left(\frac{1}{T}\right) \quad (2)$$

where T is the transmittance and d is the thickness of the crystal. Absorption coefficient (α) of the grown crystal obeys the following Tauc's relation for high photon energies (hν) [18].

$$\alpha = \frac{A(h\nu - E_g)^{\frac{1}{2}}}{h\nu} \quad (3)$$

where E_g is optical band gap of the crystal and A is a constant.

The theoretical optical band gap ($E_g = hc / \lambda$) of BGSC single crystals were premeditated to be 5.25 eV, where λ is the lower cut-off wavelength which in good agreement with the value obtained from Fig. 3.

A plot of $(\alpha h\nu)^{1/2}$ versus hν is represented in Fig.4. Using Tauc's plot the energy (E_g) is evaluated by the extrapolation of the linear part [20] and the value is determined to be 5.86 eV; the large band gap obviously designates high dielectric behaviour to induce polarization to exhibit NLO activity [19] when powerful radiation is incident on the material.

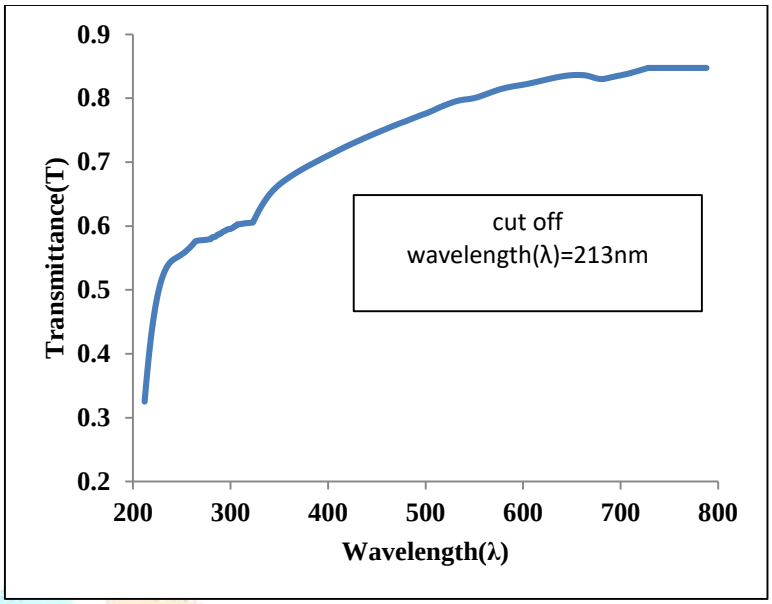

Fig. 3 Optical transmission spectrum of BGSC crystal.

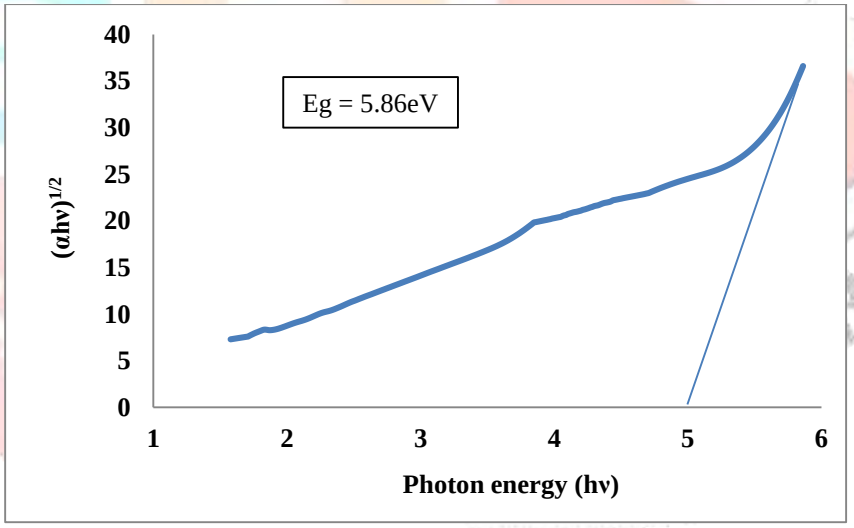

Fig. 4 Plot of $(\alpha h\upsilon)^{1/2}$ versus photon energy

3.4. FTIR analysis

In order to analyse the synthesized compound qualitatively for the presence of functional groups in the molecule, FT-IR spectral analysis was carried out in the region 4000-400cm^{-1}. It provides more information about the structure of a compound. In this technique, almost all functional groups in a molecule absorb a definite range of frequency. The absorption of IR radiation causes the various bands in a molecule to stretch and bend with respect to one another. The observed bands along with their vibrational assignments have been tabulated in the Table 3. The recorded spectrum of BGSC is shown in the Fig.5. Some of the stretching frequencies are given below. All the assignments confirm the incorporation of all constituent ions in the title compound.

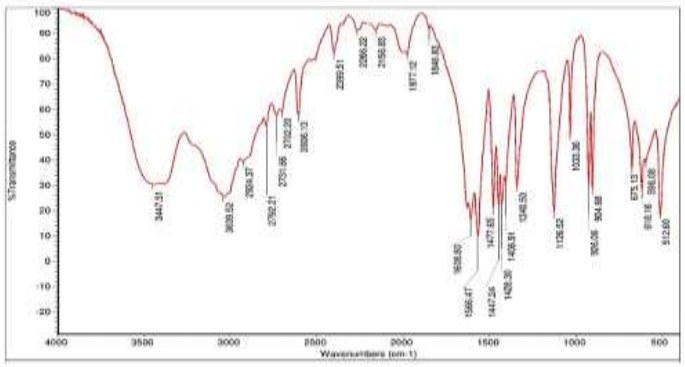

Fig.5 FTIR Spectrum of the BGSC crystal

Table 3

Vibrational Assignments of BGSC crystal

S.NO	Wavenumber (cm^{-1})	Tentative Vibrational Assignments
1	3039.52	CH stretching mode
2	2606.13	NH_3^+ group of free glycine
3	2399.51	Symmetric bending mode of NH_3^+
4	2266.22	Assymmetric bending mode of NH_3^+
5	2156.83	Assymmetric bending mode of NH_3^+
6	1608.80	NH_2^+ assymetric deformation
7	1566.47	Symmetric bending mode of NH_3^+
8	1477.65	In plane deformation of CH_2
9	1340.50	CH Stretching mode
10	1126.52	NH_3^+ group of free glycine
11	926.06	OH out of plane deformation
12	675.13	CCl stretching
13	596.08	CCl stretching
14	512.60	Presence of Carboxylate group

3.5 Dielectric studies

To study about dielectric properties of material is remarkable and requisite in almost every field such as optics, solid state, electronics and photonic device fabrications [20]. The dielectric measurement offers an opportunity to understand the electric properties of the grown crystal. Defect free, optically transparent BGSC crystal of uniform cross sectional area 3.52 × 10.69 mm^2 and thickness 4.91 mm was chosen, and its outer coated with silver paint was placed between the two copper electrodes, which acts as parallel plate capacitor. The dielectric response of a material can be concisely described as a complex quantity made up of real and imaginary components, i.e., $\varepsilon = \varepsilon' + j\varepsilon''$ where ε' and ε'' are the real and imaginary components of dielectric constant respectively. The real part characterizes the amount of energy stored by the material as a result of polarization, and imaginary component gives the energy loss by dielectric material placed in a varying electric field. Equations 11 and 12 are used to calculate the real and imaginary parts of dielectric constant of the grown crystal.

$$\varepsilon' = \frac{C\,d}{\varepsilon_0 A} \quad (10)$$

$$\varepsilon'' = \varepsilon' \tan\delta \quad (11)$$

where C is the capacitance (F), d is the thickness (m); A is the area (m^2) of the crystal, tanδ is the loss tangent and ε_0 is the absolute permittivity of the free space having the value 8.854×10^{-12} F/m.

The dielectric measurements at various frequencies are called dispersion [19]. The dielectric dispersion of the sample was noted for the applied frequency that ranging from 1 Hz to 5 MHz at different temperatures from 311 K to 401 K is shown in Fig. 6 and 7. From Fig. 7, it is observed that the dielectric constant shows normal behaviour with frequency, i.e., real part of dielectric constant decreases with the increase in frequency.

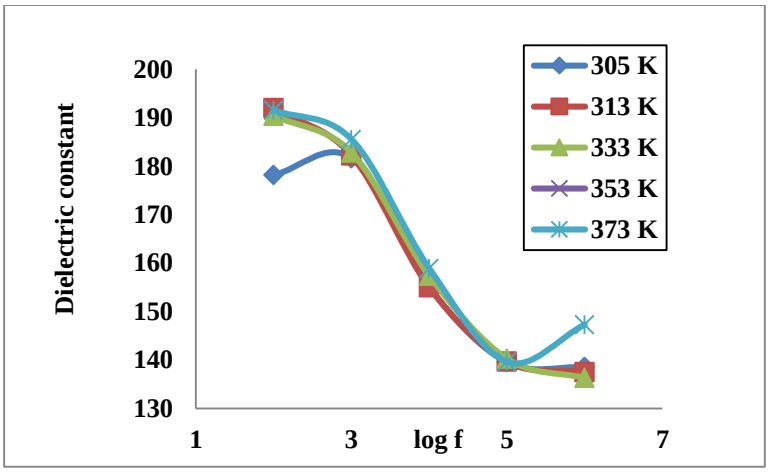

Fig. 6 Plot of dielectric loss vs. log f for BGSC crystal

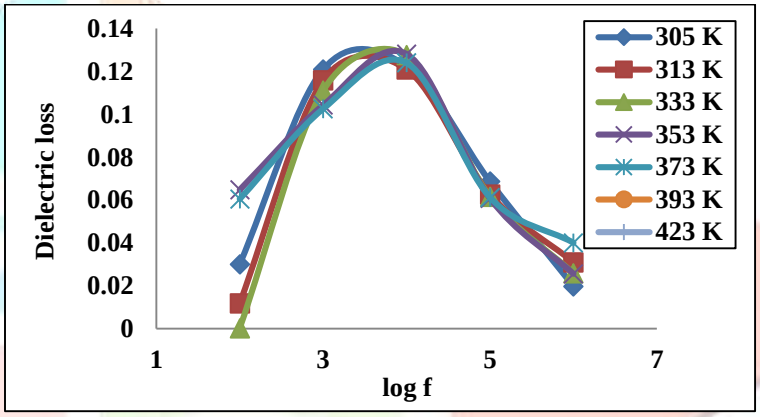

Fig. 6 Plot of dielectric constant vs. log f for BGSC crystal

The various polarizations like electronic, ionic, dipolar and space charge polarizations contribute to dielectric constant. All these polarizations are generally active at low frequencies. The low value of dielectric constant at high frequencies occurs due to the loss of these polarizations at low temperature [21]. The dielectric loss parameter characterizes the energy dissipation from the applied field into the dielectric material. This arises when polarization in the dielectric material lags behind the applied alternating field either due to the presence of impurities or crystal defects. The characteristic of low dielectric constant and dielectric loss with high frequency for a given sample proposed that the sample have superior optical quality with fewer defects and this feature is specifically vital for employing this material probable for various nonlinear optical applications.

3.5.1. Electronic polarizability (α)

The dielectric measurement is a practical tool to work out the polarizability of the medium for evaluating SHG efficiency of BGSC crystal. The dielectric constant at higher frequency (1MHz) is considered for these computations. According to the Penn model [22], the average Penn gap (E_p) and Fermi (E_F) [23] were indented by subsequent equations.

$$E_p = \frac{\hbar\omega_p}{(\varepsilon_r - 1)^{\frac{1}{2}}} \quad (4)$$

$$E_F = 0.2948\ (\hbar\omega_p)^{\frac{1}{2}} \quad (5)$$

$$\hbar = 28.8\left(\frac{Z\times\rho}{M}\right)^{\frac{1}{2}} \quad (6)$$

where $Z=[(9\times Z_C)+(7\times Z_H)+(3\times Z_O)+(2\times Z_N)+(1\times Z_K)+(1\times Z_S)\ ]=78$. Z can be worked out by substituting respective valences electrons of elements existing in the sample.

The electronic polarizability (α) of the grown material is given by the relation [24]

$$\alpha=\left[\frac{(\hbar\omega_p)^2\ S_0}{(\hbar\omega_p)^2\ S_0+3\ (E_P)^2}\right]\times\frac{M}{\rho}\times0.396\times10^{-24}\ cm^3 \quad (7)$$

where S_0 is a constant for a particular material

$$S_0=1-\left[\frac{E_p}{4E_F}\right]+\frac{1}{3}\left[\frac{E_p}{4E_F}\right]^2 \quad (8)$$

The value of α is also inveterate by using Clausius-Mosotti equations.

$$\alpha=\left[\frac{3M}{4\pi N_A\rho}\right]\left[\frac{\varepsilon_\infty-1}{\varepsilon_\infty+2}\right] \quad (9)$$

where N_A is the Avagadro number.

Considering that the polarizability is highly sensitive to the band gap, the following empirical relationship is also used to calculate α using the optical band gap of BGSC sample.

$$\alpha=\left[1-\frac{\sqrt{E_g}}{4.06}\right]\times\frac{M}{\rho}\times0.396\times10^{-24}\ cm^3 \quad (10)$$

where E_g is the band gap, M is the molecular weight and ρ is the density of BGSC crystal.

The calculated parameter of electronic polarizability (α) of BGSC is higher than the standard KDP [25] and the values are scheduled in Table 4 proves that the polarizability enhances the efficiency of SHG and THG of the material.

Table 4

Comparison of Theoretical measurements of BGSC crystal with KDP

Parameters	Values of BGSC	Values of KDP [29]
Plasma energy(eV)	20.07	17.29
Penn gap(eV)	1.72	0.3458
Fermi energy(eV)	17.09	13.18
Electronic polarisability by Penn gap analysis(cm^3)	7.286×10^{-23}	2.14×10^{-23}
Electronic polarizability by Clausius-Mosotti equation(cm^3)	7.27×10^{-23}	2.14×10^{-23}
Electronic polarizability by using band-gap (cm^3)	6.99×10^{-23}	-

3.6. Mechanical studies

Microhardness studies directly correlates with crystal struture, and is very accessible to the presence of any other phase transition and lattice perfections prevalent in the system. Hardness of the material is a computation of resistance it offers to local deformation or damage under an applied stress [26] and it plays a significant role in device fabrication. A transparent, smooth and flat surface of the grown BGSC crystal was subjected to hardness study at room temperature with the load ranging from 25-100g using Vicker's hardness. The indentation time was kept as 5s for all the loads. The Vickers microhardness number was calculated using the relation,

$$H_v=1.8544\left(\frac{P}{d^2}\right)\ kg/mm^2 \quad (11)$$

where P is the indenter load and d is the diagonal length of the indentation marks in mm. A plot obtained between the hardness number (H_v) and the applied load (P) is depicted in Fig.7. According to normal indentation size effect, the hardness of the crystal decreases with increasing load and but in present study the hardness of the grown BGSC crystal shows reverse indentation

effect(RISE) [27], indicates the behaviour of increase in hardness number with increasing load. In accordance with traditional Meyer's law, the relation connecting the applied load logP and size d, is given by [28].

$$P = K_1 d^n, \quad (12)$$

and K_1 is the standard hardness value and n is the Meyers index or working hardening coefficient. The plot of log P versus log d for BGSC crystal is shown in Fig. 8, yields a straight line and from the slope, the work hardening exponent n is found to be 2.607. As per Onitsch [29], the materials having workhardening exponent $1 \leq n \leq 1.6$ are hard materials and $n > 1.6$ are soft materials. Since in the present investigation the n value is 2.607, BGSC belongs to soft category material.

In view of the fact, the material takes some time to revert to elastic mode, for every indentation a correction x is applied to the d value and Kick's law is related as

$$P = K_2 (d+x)^2 \quad (13)$$

$$(\text{i.e}) \; d^{\frac{n}{2}} = \left(\frac{K_2}{K_1}\right)^{1/2} d + \left(\frac{K_2}{K_1}\right)^{1/2} x \quad (14)$$

Figure. 9 indicates the plot of load versus (diagonal length)^n. For the grown crystal, the plot $d^{\frac{n}{2}}$ versus d shown in Fig.10 gives slope $\left(\frac{K_2}{K_1}\right)^{1/2}$, the intercept is a measure of x. The striking factor x is positive only when $n < 2$ and negative for $n > 2$ and it is proved in our case.

The fracture toughness exhibits, the amount of fracture stress is applied under uniform loading for a crystal with well-defined crack, resistance to fracture indicated the toughness of a material. As per Ponton and Rawlings in 1989, two types of crack systems exist in a material as a result of indentation. The radial-median($C/a \geq 2.5$) and Palmqvist($C/a \leq 2.5$) crack systems. Transtion from Palmqvist to median crack occurs at a well-definge value of C/a, the crack length C is measured from the centre of indentation mark to the crack end it is the average of two crack lengths for each indentation $C \geq \frac{d}{2}$ [30].The nature of crack system developed in BGSC is radial-median and the fracture toughness (K_c) [31]is given by

$$K_c = \frac{P}{\beta C^{3/2}} \quad (15)$$

where P is the applied load and β the geometrical constant and the value is equal to 7 for Vickers indenter and the value of K_c is specified in Table 5. Brittleness index(B_i) is the another property which affects the mechanical behaviour of the grown crystal, deals about the fracture induced in a material without any appreciable deformation. and is computed using the realation [32],

$$B_i = \frac{H_v}{K_c} \quad (16)$$

For the hardness value, the yield strength(σ_v) was found out using

$$\sigma_v = \frac{Hv}{2.9}(1-(2-n))\left[\frac{12.5(n-2)}{1-(n-2)}\right]^{n-2} \quad (17)$$

The elastic stiffness constant(C_{11}) were calculated for the title compound using Wooster's empirical relation [33] is given by

$$C_{11} = H_v^{\frac{7}{4}} \quad (18)$$

The mechanical parameters like K_1, K_2, H_v, K_c, B_i, σ_v and C_{11} were tabulated in Table 6 and it is verified from C_{11} (first order coefficient) that the binding forces between the ions are resonably tough and the mechanical strength of material was determined to be adequately large enough to withstand the stresses set up internally in the material.

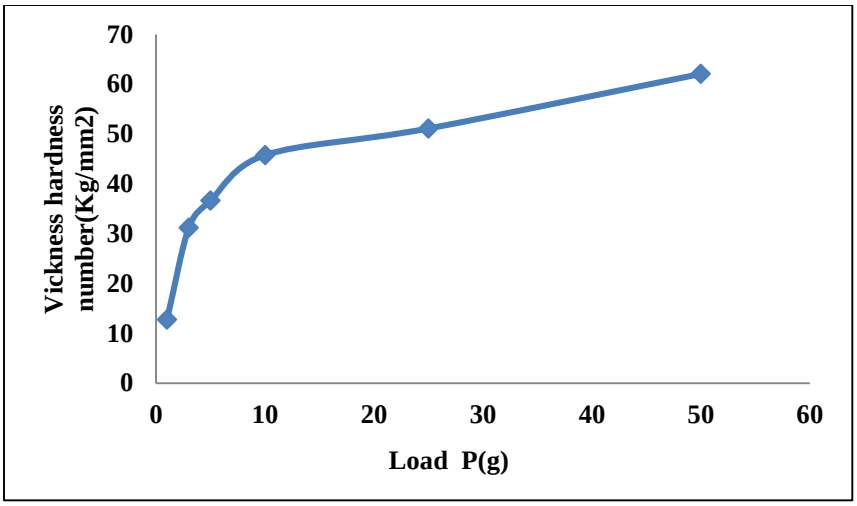

Fig. 7 Plot of Vickers's hardness versus load of BGSC crystal

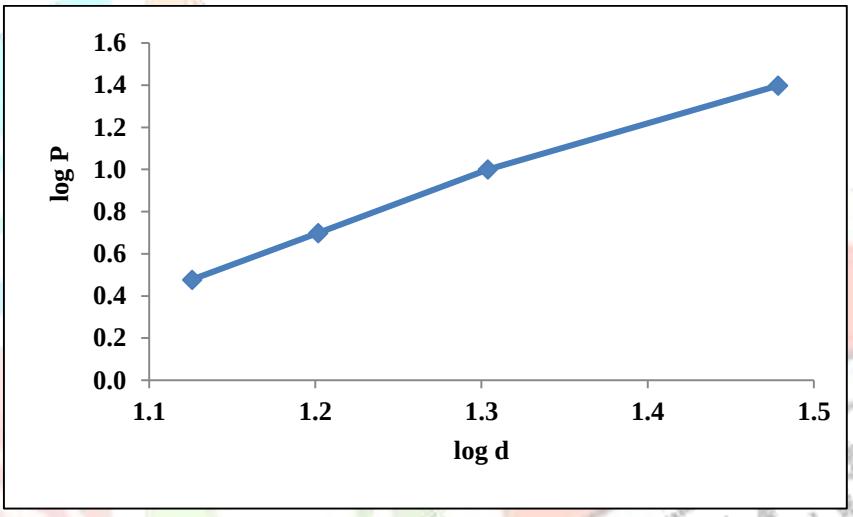

Fig. 8 Plot of log P versus log d

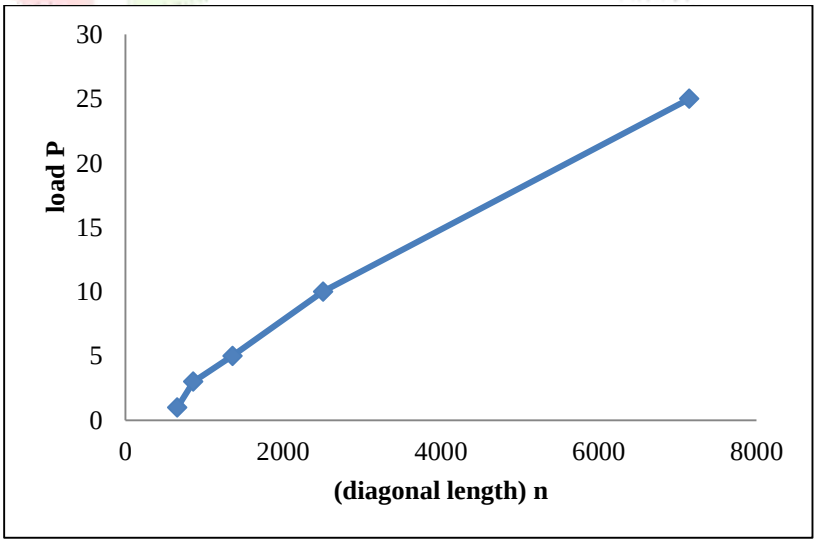

Fig. 9 Plot of load versus (diagonal length)^n

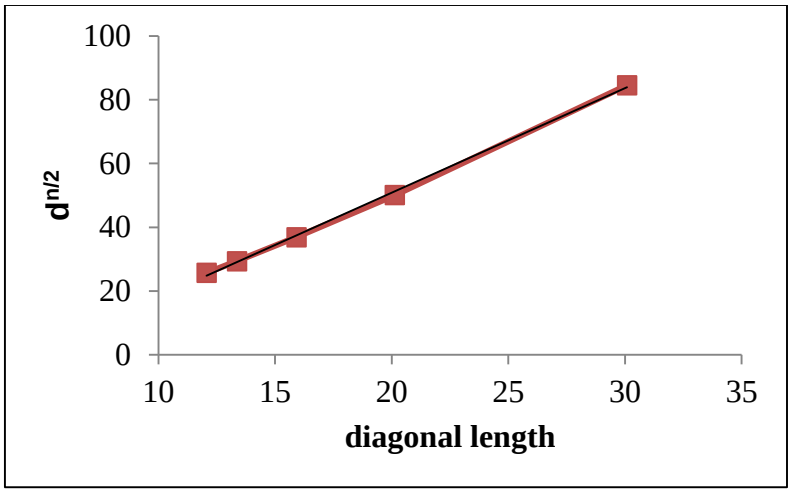

Fig. 10 Plot of (diagonal length)$^{n/2}$ versus diagonal length .

Table 5

Mechanical parameters of BGSC crystal

Parameters	Values
n	4.0783
K_1 (kg mm^{-1})	0.003
K_2 (kg mm^{-1})	0.091
H_v (kg mm^{-2})	37.405
x (µm)	-48.762
K_c (MN m$^{-3/2}$)	0.303833
B_1 (m$^{-1/2}$)	2312.37
σ_v (M Pa)	555
C_{11} (10^{14}Pa)	40

Table 6

Vickers haradness number, and Stiffness constant for vaious loads

Load P	d (mm)	H_v (kg/mm^2)	$C_{11} \times 10^{14}$ Pa
3	10.885	18.77	16.9
5	14.785	24.57	27.1
10	23.995	37.99	58.1
25	54.425	83.85	232.3
50	77.195	104.39	340.9

100	130.14	160.28	722.0

IV.CONCLUSIONS

Optically transparent high-quality innovative nonlinear optical BGSC crystals with enhanced have been profitably synthesized by slow evaporation technique at room temperature and the single crystal x-ray diffraction studies validate the orthorhombic structure with space group Pbcm. CHN analysis substantiates the purity of the crystal. UV-Vis spectrum outstandingly reveals the inherited transparency of the crystal in the entire visible region, with lower cut-off wavelength 213 nm and by using Tauc's plot the optical band gap value was recognized to be 5.25 eV. The higher value of dielectric constant with low loss concludes that the title crystal is more pertinent candidate for optoelectronic and NLO applications. Prediction of solid state physical parameters discloses that the electronic polarizability of BGSC found to be superior to KDP. The Vickers hardness divulges the soft nature and reverse indentation size effect (RISE) of title compound. The end results obtained from various studies recommend that the presence of Strontium chloride enhance the properties of BGSC crystals and consequently make it fit for the device fabrication like optical limiting and photonic devices.

Acknowledgements

The authors would like to express their sincere gratitude to SAIF, Kochi for extending instrumentation facilities. The authors also thank SAIF, IIT Madras for single crystal XRD and DSC analysis. The authors also grateful to Dr. S. Jerome Das, Department of Physics, Loyola College for providing dielectric and micro hardness facilities.

References

[1] D. Prem Anand, M. Gulam Mohamed, S.A. Rajasekar, S. Selvakumar, A. Joseph Arul Pragasam, P. Sagayaraj, Growth and characterization of pure, benzophenone and iodine doped benzoyl glycine single crystals. Mater.Chem.Phys. 97 (2006) 501-505.

[2] M.D. Shirsat, S.S. Hussaini, N.R. dhumane, V.G. Dongre, Influence of lithium ions on the NLO properties of KDP single crystals, Cryst. Res. Technol. 43(7) (2008) 756-761.

[3] S.S Hussaini. N.R.Dhumane, V.G.Dongre.P.Karmuse, P.Ghughae, M.D.Shirsat, J.Opt.Elect.Adv.Mater. (RapidCommun). 1 (2007) 707-711.

[4] B. Ruiz, M. Jazbinsek, P. Gunter (2008), Crystal growth of DAST, Cryst Growth and Design. 8(11) (2008) 4173 – 4184.

[5] Lenin, M., M. Chandrasekar, and G. Udhayakumar. "Growth and characterization of nonlinear optical single crystal: Glycine zinc sulfate." *International Journal of ChemTech Research* 6.5 (2014): 2683-2688.

[6] Acharya, P. Kumara, and P. S. Narayanan. "Raman and infrared spectra of ferroelectric(CH3NH2CH2COO) 3 CaCl2." *Journal of Raman Spectroscopy* 1, no. 5 (1973): 499-505.

[7] Helina, B. "Synthesis, Growth and Characterization of semi-organic non-linear optical Triglycine phosphoric acid (TGPA) single crystals." *JOURNAL OF ADVANCED APPLIED SCIENTIFIC RESEARCH* 1.9 (2017).

[8] Selvaraju, K., Valluvan, R., & Kumararaman, S. (2006). New nonlinear optical material: Glycine Hydrofluoride. *Materials letters*, *60*(23), 2848-2850.

[9] Nagaraju, D., Shekar, P. V., Rao, T. B., & Rao, K. K. (2013). Growth, Defects and Hardness Studies on Diglycine Barium Chloride Monohydrate Crystals. *Advanced Science Focus*, *1*(2), 129-135.

[10] Dillip, G. R., et al. "Crystal growth and characterization of γ-glycine grown from potassium fluoride for photonic applications." *Spectrochimica Acta Part A: Molecular and Biomolecular Spectroscopy* 79.5 (2011): 1123-1127.

[11] Moolya, B. N., Jayarama, A., Sureshkumar, M. R., & Dharmaprakash, S. M. (2005). Hydrogen bonded nonlinear optical γ-glycine: Crystal growth and characterization. *Journal of crystal growth*, *280*(3-4), 581-586.

[12] Balaji, S. R., Balu, T., & Rajasekaran, T. R. (2018). Single-crystal growth, structure refinement and the properties of Bis (glycine) Strontium Chloride. *Materials Research Express*, *5*(2), 026205.

[13] S. Anie Roshan, C. Joseph, M.A. Ittyachen, Mater. Lett. 49 (2001) 299.

[14] V. Venkataramanan, S. Maheswaran, J.N. Sherwood, H.L. Bhat, J. Cryst. Growth 179 (3–4) (1997) 605

[15] D.D.O. Eya, A.J. Ekpunobi, C.E. Okeke, Academic Open Internet J. 17 (2006).

[16]V. Pandey, N. Mehta, S.K. Tripathi, A. Kumar, Chalcogenide Lett. 2 (2005) 39.

[17]Optoelectrons by E.Rosencher.

[18] Tauc J, Grigorovici R, Vancu A. Optical properties and electronic structure of amorphous germanium. Phys Status Solidi.1966;15:627–37.

[19] P.S. Latha Mageshwari, R.Priya, S.Krishnan, V.Joseph, S.Jerome Das, Growth, optical, thermal, dielectric, and mechanical studies, of sodium hydrogen succinate single crystal. A third order NLO material ,J Therm Anal Calorimetry 128(2017)(1),29-30.

[20] Shkir, M.; Muhammad, S.; AlFaify, S.; Chaudhry, A. R.; Al-Sehemi, A. G. Shedding Light on Molecular Structure, Spectroscopic, Nonlinear Optical and Dielectric Properties of Bis (Thiourea) Silver (I) Nitrate Single Crystal: A Dual Approach. *Arab. J. Chem.***2016.**

[21] M.Dongol Egypt, J.Solids 25 (2002) 33.

[22]D.R. Penn, Wave-number-dependent dielectric function of semiconductors , Phys. Rev.128 (1962) 2093–2097.

[23]C. Balarew, R. Duhlew, Application of the hard and soft acids and bases concept to explain ligand coordination in double salt structures, J. Solid State Chem. 55 (1984) 1–6.

[24] N.M. Ravindra, V.K. Srivastava, Electronic polarizability as a function of the penn gap in semiconductors, J. Infrared Phys. 20 (1980) 67–69.

[25] R. Robert, C.JustinRaj, S.Krishnan, S.JeromeDas, Growth, theoretical and optical studies on potassium dihydrogen phosphate (KDP) single crystals by modified Sankaranarayanan–Ramasamy (mSR) method Physica B 405 (2010) 20–24.

[26] BW. Mott, in: MicroIndentation Hardness Testing, Butterworths, London, 1956, p. 206.

[27] K. Sangwal, On the reverse indentation size effect and microhardness measurement of solids, Mater. Chem. Phys. 63 (2000) 145–152.

[28] E. Meyer, Untersuchungen über Härteprüfung und Härte Brinell Methoden, Z.Ver. Deut. Ing. 52 (1908) 645–835.

[29] Onitsch EM. The present status of testing the hardness of materials, *Microscope* .1950; 95:12.

[30]Suresh Sagdevan,R.Varatharajan,Int.J.Phys.Sci.8(39)(2013)1892–1897.

[31] Banwari Lal, K.K. Bamazai, P.N. Kotru, B.M. Wanklyn, Mater. Chem. Phys. 85 (2004) 353.

[32] K. Nihara, R. Morena, D.P.H. Hasselman, Evaluation of KIc of brittle solids by the indentation method with low crack-to-indent ratios, J. Mater. Sci. Lett. 1(1982) 13–16.

[33] W.A. Wooster, Physical properties and atomic arrangements in crystals, Rep. Prog. Phys. 16 (1953) 62–82.